SAE TECHNICAL PAPER SERIES

940236

Flow Characteristics of SiC Diesel Particulate Filter Materials

S. C. Sorenson and Jakob W. Høj
Technical University of Denmark

Per Stobbe

Reprinted from: Diesel Exhaust Aftertreatment 1994
(SP-1020)

SAE The Engineering Society For Advancing Mobility Land Sea Air and Space® INTERNATIONAL

International Congress & Exposition
Detroit, Michigan
February 28-March 3, 1994

400 Commonwealth Drive, Warrendale, PA 15096-0001 U.S.A. Tel: (412)776-4841 Fax:(412)776-5760

940236

Flow Characteristics of SiC Diesel Particulate Filter Materials

S. C. Sorenson and Jakob W. Høj
Technical University of Denmark

Per Stobbe

ABSTRACT

Recent studies have shown that SiC provides substantial advantages for use as the material for wall flow diesel particulate filters. In addition to very advantageous thermal properties, it has been shown that SiC based filter material has higher permeability than Cordierite.

This paper presents a comparison of the basic flow characteristics of SiC based and Cordierite based wall flow filter material, expressed in terms of parameters which are basic materials properties that are independent of filter geometry.

In addition, the flow characteristics of the particulate matter collected on the filter during engine operation are presented. The results show that the advantageous flow characteristics observed with the basic filter material are retained for loaded filters, up to very high loadings.

INTRODUCTION

In order to reduce the problems associated with damage to diesel particulate filters during regeneration, many systems have been developed to carefully control conditions in filters during regeneration. In a large number of these systems, the filter elements have been made of a honeycomb structure of porous Cordierite with plugged ends. Due to a low melting point and a low thermal conductivity, problems often arise with local temperatures approach the melting temperature of Cordierite.

A material which has very attractive properties for reducing this problem is Silicon Carbide (SiC). In particular, its high decomposition temperature and high thermal conductivity make it specially attractive with respect to withstanding very severe regeneration conditions.

Recent work has shown that it is possible to construct wall flow filters out of SiC, and that these filters have many desirable properties (1-4). In addition to the thermal properties, SiC wall flow filters have been found to have desirable flow characteristics, and give lower pressure losses under comparable conditions.

It is the purpose of this paper to further investigate the flow characteristics of SiC filter material and compare them to those of Cordierite. In making this comparison, an attempt has been made to make the characterization on the basis of theoretically based considerations and material parameters, so that the results can be used in a general fashion and not specific to a given filter configuration.

Two aspects of the flow characteristics are considered. The first is the flow pressure drop relation of the basic material itself in the unloaded form. The second is that of the loaded filter. This is an important aspect of the problem, since for reasonable filter loadings, it is the particulate matter which essentially determines the pressure drop through the filter.

FILTER MATERIAL

PROPERTIES

Two materials were used in the investigation: a material based on SiC particles joined strongly together (1), and a Cordierite structure, commonly referred to as EX-66. Photographs of the structures of the SiC and Cordierite materials are given in Figure 1 and 2, and show that they have quite different structures. The photographs indicate a more uniform structure for the SiC, and the absence of the very large pores which are observed in the Cordierite structure. Many of these large pores appear to be closed, and would not contribute to the flow area. In another study, it has also been shown that SiC materials have a much more uniform pore size than Cordierite (2).

A summary of the most important properties of the filter materials used is shown in Table 1. The SiC material has a slightly higher porosity and a slightly larger mean pore size than the Cordierite material. The SiC material also has a thicker wall and a smaller filtration area than the Cordierite. A more complete description is given in Reference (1) for SiC filters. For the Cordierite material, values were obtained from Reference (5).

Property	SiC	Cordierite
Bulk Density - g/cm^3	1.6	1
Porosity - %	50	43 - (5)
Cells per cm^2	8	16
Cell size, mm	3.5x3.5	2.54x2.54
Wall thickness -mm	1	0.635
Surface area - m^2/l	0.42	0.63
Mean pore size - μm	40	33 - (5)
Permeability - Darcy	2.1	0.64

Table 1. Properties of the filter materials used in the study.

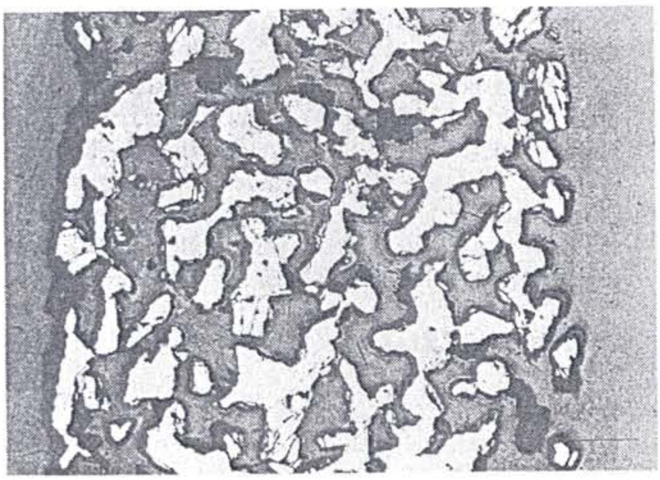

Figure 1. A photograph of the cross section of the SiC filter material. The wall thickness is 1 mm. The black areas are voids in the epoxy bonded to the SiC material.

FLOW THROUGH FILTER MATERIAL

In the following, reference will be made to some geometrical parameters for wall flow filters. Figure 3 shows the variables used and the nomenclature. The width of the honeycomb cell is denoted by a, the wall thickness by t, and the length of the entire filter by L. In addition, there are two velocities that are used. The first, denoted by v, is the so called face velocity,

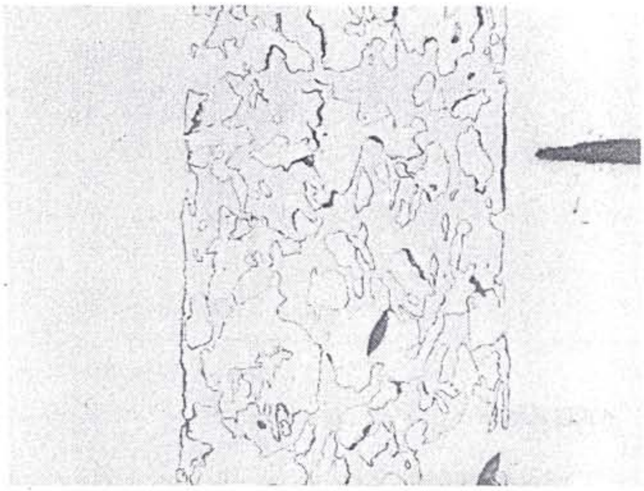

Figure 2. A photograph of the cross section of the Cordierite filter material. The wall thickness is 0.63 mm. The black areas are voids in the epoxy bonded to the Cordierite material.

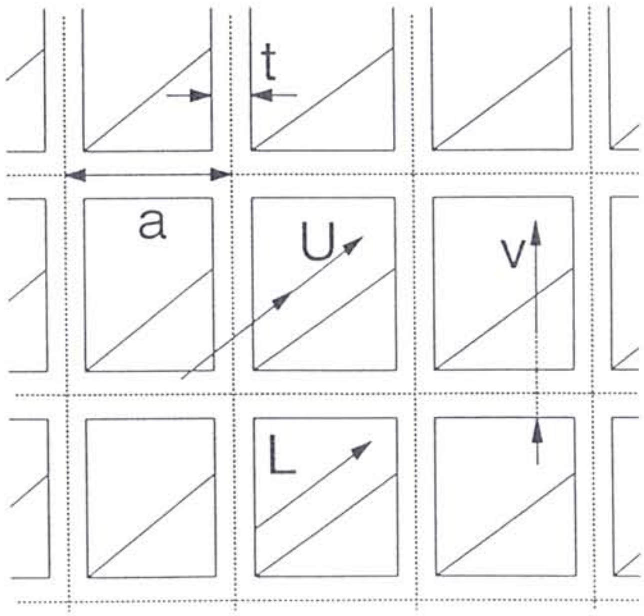

Figure 3. Nomenclature used for the wall flow filter structure.

that is the velocity of the gas as it enters the filtration surface. The second velocity is denoted by U. It is the entrance velocity at the open end of the filter channels.

For proper flow conditions, it can be expected that the flow through the filter material will obey Darcy's law, given in Equation 1:

$$dp = \frac{v \cdot \mu \cdot t}{\alpha} \quad (1)$$

where: dp is the pressure drop, μ is the gas viscosity, and α is the permeability of the porous media. Dullien (6) gives an approximate limit for the region where Darcy's law begins to deviate from linearity as a Reynolds number on the order of from 1 to 10.

$$Re_1 = \frac{v \cdot D_p \cdot \rho}{\mu} \quad (2)$$

In Equation 2, the Reynolds number is defined on the basis of a "surface average" sphere diameter D_p for the particles in the porous media, ρ is the gas density, and μ is the gas viscosity.

A deviation from Darcy's law can be seen either from a deviation from linearity in the relationship between the flow and pressure drop relation from Equation (1), or in more general terms, in a logarithmic plot of the friction factor as a function of the Reynolds Number. In Dullien (8), the friction factor is defined as:

$$f = \frac{dp}{\rho \cdot v^2} \cdot \frac{D_p}{t} \quad (3)$$

It is the filter wall material itself that would be expected to be the most likely to deviate from Darcy's law. For a given flow rate and density entering the particle layer, the difference between the Reynolds numbers for the filter material and the particle layer will be solely due to the difference in the diameter of the particles. For the exhaust particles, typical sizes are on the order of 1 μm (7), while for typical wall flow filter materials particle/pore sizes will typically range from 10 to 100μm. Therefore, the Reynolds number for the filter wall material will be at least an order of magnitude higher than that of the particle layer consisting of diesel particulate matter.

EXPERIMENTAL RESULTS

In order to determine the flow characteristics of the filter materials, tests were conducted in a simple cold flow bench. Air was directed through a filter body by using a series of centrifugal blowers, and the pressure drop was monitored as a function of flow rate. This setup was also used for some measurements with loaded filters, but the blowers could not deliver the high pressures needed to provide the high flow rates found under engine conditions. Cold flow measurements of loaded filters did, however, provide a supplement to the higher flows during engine operation, and provided accurate flow and pressure measurements at lower flow rates.

For all measurements, the pressure drop was taken to be solely due to the effect of the gasses flowing through the porous wall and in the event of a loaded filter, through the particle layer and wall of filter material itself. This was justified by using the theoretical considerations developed in References (8) and (9). Using the model of Reference (8), it was determined that the pressure drop due to the flow along the length of a filter channel was insignificant. Similarly, using the techniques given in Reference (9) it was found that end losses also were insignificant.

In Reference (1), flow data were presented for SiC and Cordierite structures with comparable porosities and mean pore sizes for flow velocities up to 5 cm/sec. The pressure drop was found to be a linear function of the linear flow velocity for both materials. In order to find a point where a deviation from Darcy's law occurred, a series of tests were conducted on the cold flow bench at higher velocities of up to 15 cm/s for the Cordierite material, and 20 cm/s for the SiC. These results are shown in Figure 4, where it can be seen that at flows over about 5 cm/s, the relation between the pressure drop and the flow velocity becomes non-linear Also shown in Figure 4 are lines representing the linear behavior measured in Reference (1).

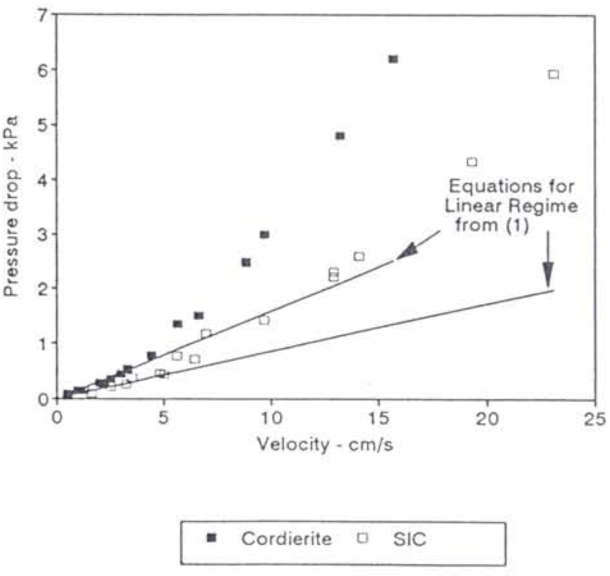

Figure 4. Pressure drop as a function of face velocity for the two filter materials.

The permeability of the two materials can be determined from the slope of the curves in Figure 4. For the SiC, the permeability is 2.1×10^{-12} m^2 = 2.1 Darcy, and for the Cordierite the permeability is 0.63 Darcy. Additional measurements on small discs of a Cordierite type EX-47 material gave a permeability of 0.22 Darcy. The measured value for the EX-66 Cordierite is lower than the results of Reference (8) who reported a value of 1 Darcy based on theoretical conversion of the measured value of 0.2 Darcy for EX-47 type material, but the measured value for the EX-47 is very good agreement with Reference (8).

CORRELATION OF DATA

Empirical results for flows through idealized porous structures follow the following relationship between Reynolds number and the friction factor in the region where Darcy's law is valid:

$$f = \frac{K}{Re} \tag{4}$$

where: K is an empirical constant that has been found to be a function of porosity, surface roughness, tortuosity, etc. (6). From the definitions of the friction factor and Reynolds number, it can be shown that Equation (4) implies the following relationship between the permeability and the surface average particle diameter:

$$\alpha = K \cdot D_p^2 \tag{5}$$

This is a useful relationship, since it can be used to establish an equivalent diameter for the particles of a porous structure through a simple measurement of the permeability of a structure. In the case of Cordierite, it is very difficult from a strictly geometrical point of view to establish this parameter.

Equation (5) can then be used to calculate equivalent particle diameters based on permeability, but some reference condition is needed to establish the constant K in Equation (5). For the work presented here, the following procedure was used. Since the structure of the SiC filter is based on grains with a known and fairly uniform size, the permeability of the SiC material was used to determine K. From this value of K and the permeabilities of the Cordierite filter materials, equivalent diameters for the Cordierite materials were then established. The results are given in Table 2

When discussing the equivalent diameters, it should be remembered that they are based on a relationship developed from SiC material. Because the structure of the Cordierite tends to be that of pores inside of a more solid material, it is difficult to give a definite physical significance to the equivalent particle diameter. The use of the equivalent diameter is, however, a way to bring the permeability into the standard parameters of the friction factor and the Reynolds number, and is in fact equivalent to defining these two parameters on the basis of the square root of the permeability instead of an actual physical dimension.

Property	SIC	EX-66	EX-47
Porosity	50	43	50
Mean Pore size -μm	40	33	13
Permeability - Darcy	2.1	0.63	0.22
Equivalent Diameter - μm	80	44	36

Table 2. Flow size and flow resistance data for three types of filter material.

In a study of flow through EX-47 type Cordierite filters Mogaka et. al. (9) established the following relationship between a non-dimensional pressure drop and a Reynolds Number. The nondimensional pressure drop they used is defined as:

$$dp^* = \frac{dp}{\rho \cdot U^2 / 2} \tag{6}$$

In addition, the Reynolds number used in Reference (7) was based on the cell width.

$$Re_2 = \frac{U \cdot a \cdot \rho}{\mu} \tag{7}$$

The formulations used in Equations (6) and (7) are acceptable where the length of the filter bodies is constant, but for conditions where filters of different length are to be compared, the formulation of Equations (2) and (3) should be used, since it is in general terms and the length of the filter is part of the definition of the friction factor.

For filters with square channels as shown in Figure 3, the relationships between the formulations from Dullien (6) and Mogaka et. al (9), follows:

$$dp^* = \frac{f \cdot (a - w)^2 \cdot w}{8 \cdot D_p \cdot L^2} \tag{8}$$

$$Re_2 = Re_1 \cdot \frac{4 \cdot L \cdot a}{D_p \cdot (a - w)} \tag{9}$$

Based on these relationships and using the value of the equivalent diameter for the EX-47 material from Table 2, the correlation between the non-dimensional pressure drop and Reynolds number given in Reference (9) can be converted to the formulation in terms of the parameters given in Dullien (6) as follows:

$$f = 2840 \ Re_1^{-1.06} \qquad (10)$$

The results from the flow tests on the Cordierite and SiC filter materials shown in Table 1 are given in Figure 5, along with a plot of Equation (10). It should be noted that in Reference (9), the results presented do not include data points for $Re_2 > 9000$ ($Re_1 > 0.2$), and so it is not known what is the maximum Reynolds number for which the correlation is valid.

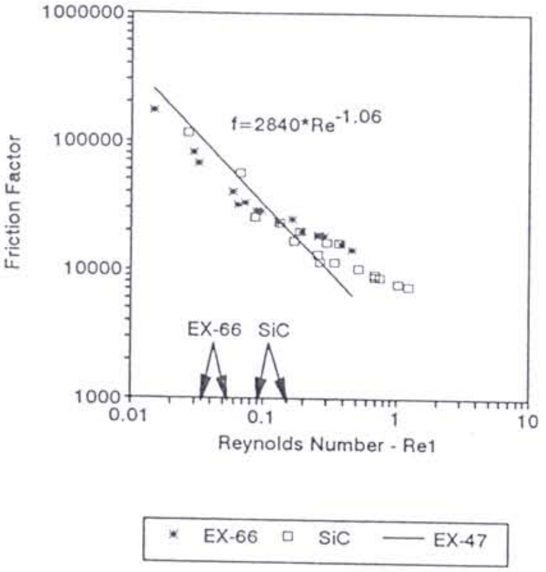

Figure 5. Friction factor as a function of Reynolds number for SiC and Cordierite filter materials.

Also shown in Figure 5 are the ranges of Reynolds numbers encountered for the filter materials in the engine tests with loaded filters in this study. Reference (6) also gives a relation of the same form as Equation (10) for flow through a packed bed of glass beads. The power of the Reynolds number was 1.0 which is close to the value for Equation (10), and the coefficient was given in terms of the porosity. When using the porosity correction given in Reference (6), the coefficient was found to be about 1/10th of that in Equation 10.

There are at least two factors which can affect this coefficient. The first is, as mentioned, the porosity. Reference (6) lists a large number of different corrections which try to account for the effect of porosity. Some of these vary considerable. The second is the coefficient from Reference (6) is apparently for liquids, while the results presented here are for gasses. It is know that gasses can behave somewhat differently in porous structures than liquids.

For the measurements of this study, it can be seen that there is a region at low Reynolds numbers where the same functional relationship holds as for Reference (6), and that the values are nearly the same as those given by Equation (10). At a Reynolds number of about 0.2, the data points begin to show a deviation from the straight line, and the Cordierite data points lie above those for the SiC.

Initially, Figure 5 would seem to imply that the materials are all equivalent. However, upon consideration of the definitions for the friction factor and the Reynolds number, which include the equivalent particle diameter, it can be shown that the curves are actually another way of expressing the permeability, since the equivalent diameter is proportional to the square root of the permeability.

Take, for example, the conditions for two filters with the same filtration area and thickness operating in engine exhaust at the same engine operating condition. If the back pressure is low, then the gas densities will be the same and therefore the face approach velocities will also be the same. The Reynolds numbers will not be the same, however, if the two filters have different equivalent diameters (i.e. permeabilities). The filter with the smallest equivalent particle diameter (lowest permeability) will have the lowest Reynolds number, since other variables determining the Reynolds number will be the same. This filter will then have a higher friction factor. In the region where Darcy's law is valid the friction factor will be inversely proportional to the equivalent diameter. Since the pressure drop is also inversely proportional to the equivalent particle diameter, this filter material will then have the greatest pressure drop. The ratio will be determined by the ratio of the squares of the equivalent diameters, i. e. the permeabilities.

To sum up, the reason that the materials appear to have the same flow characteristics in the region of Figure 5 where the friction factor is inversely proportional to the Reynolds number, is that they all obey Darcy's law, and the equivalent diameters are determined from Equation (5), which is a result of Darcy's law. If the materials obey Darcy's law, then the permeability of the material itself gives a complete description of the pressure loss characteristics of the material itself. Effects of filter area and thickness can then be determined through determination of face velocities and application of Darcy's law.

PARTICLE LAYERS

BASIC CONSIDERATIONS

In the previous section, it was shown that for materials which obey Darcy's law, it is only necessary to determine the permeability to determine the pressure drop characteristics. As indicated by Figure 5, one would expect the particle layer to follow Darcy's law because the typical diesel particle size is much smaller than the equivalent diameters given in Table 2. Therefore, the effort concerning particle layer pressure loss characteristics will be concentrated on determining the permeability of the particles on the filter.

For determining the pressure loss characteristics of the particle layer it was assumed that the pressure drop through a loaded filter is the sum of two contributions: the pressure drop through the filter material itself, as discussed previously, and the pressure drop due to the particles. Since the pressure loss characteristics of the basic materials have been established, the pressure drop through the filter material can be calculated as a function of the face velocity (flow rate and density) and the viscosity of the gasses (temperature) and then subtracted from the total pressure drop over the filter. The two contributions to the pressure drop were assumed to be independent. This is not to say that the filter material does not have an effect on the properties of the filter layer, but it attributes all changes in pressure drop characteristics apart from changes in the viscosity and velocity through the filter material to the accumulation of particles.

The next assumption is that Darcy's law holds for the particle layer. This has been discussed at the beginning of this section. As an additional indication that this is the case is given by some cold flow bench experiments on loaded filters. Filters were loaded with different weights of particles and the pressure drop was determined as a function of face velocity. With the

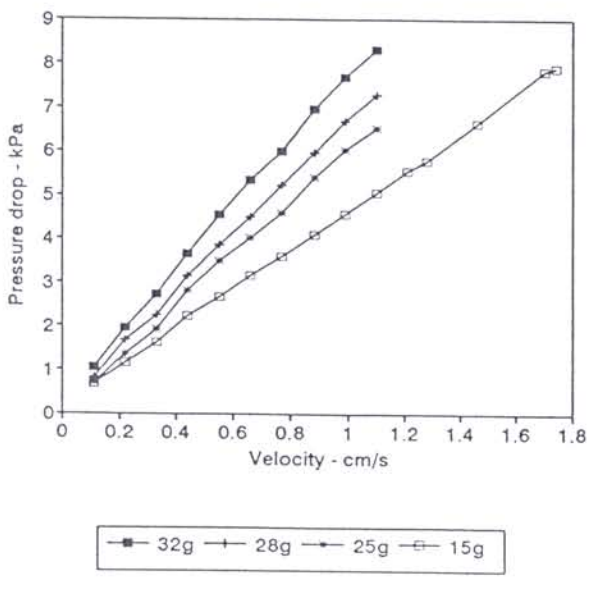

Figure 6. Pressure drop as a function of face velocity for cold flow bench test of a loaded SiC particle filter.

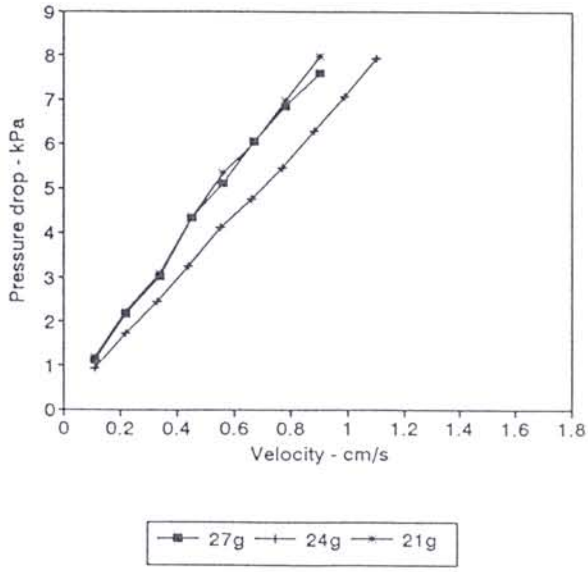

Figure 7. Pressure drop as a function of face velocity for cold flow bench test of a loaded Cordierite particle filter.

loadings encountered, the maximum pressure drop for both the clean SiC and Cordierite filters is about 0.14 kPa. For the flow conditions used, it has been shown that the basic filter material obeys Darcy's law. Therefore, any deviation from linearity of flow relationships for loaded filters would reflect a deviation from Darcy's law.

Figures 6 and 7 show the pressure drop across the particle layer as a function of the face velocity for these experiments. It can clearly be seen that in this region,at least, there is a linear relationship between the velocity and pressure drop, indicating that Darcy's law is applicable here.

The thickness of the particle layers for the conditions shown was determined to be about 0.2-0.4 mm. This is about one half the wall thickness for the filters, and the pressure drops are about 50 times those of the filter material. This implies that the permeability of the filter material is on the order of 200 times greater than that of the particle layer, and that an equivalent diameter of the particles in the layer would be about an order of magnitude lower than those of the filter materials. This is 2-5 μm, which is somewhat larger than values reported in the literature for diesel particulate matter (7), but it is of the correct magnitude. The Reynolds numbers for the particle layers would then be an order of magnitude less than those of the filter materials previously determined. The agreement of the above equivalent diameter with known diesel particle diameters also indicates that the particulate matter on the filter behaves similar to Figure 2. Since the velocities are essentially the same through the filter and the base material, then the Reynolds numbers for the particle layer should be an order of magnitude lower than those of the base material, and as indicated from Figure 2, well into the region where Darcy's law will be valid.

In Darcy's law as given in Equation (1), it is necessary to know the thickness of the particle layer. This is very difficult to measure directly because a filter must be dismantled and, in fact, destroyed to make physical measurements throughout the filter structure. Even so, the handling process may disturb the particle layer, affecting results. The particles first collected may also penetrate into some of the filter structure, making it difficult to physically determine a thickness.

As an alternative to actually measuring the thickness, the concept of an effective particle thickness was used. The assumptions made are that the particles are evenly distributed over the entire face of the filter, and that there is, in effect, a sharp boundary between the particles and the filter material. Since the filter materials are porous, this assumption may not be very accurate, especially in the first stages of particle collection. As in the case of the effective particle diameter in connection with the permeability, one then is concerned with an effective thickness of the particle layer.

Under these assumptions, the effective thickness of the particle layer, δ is:

$$\delta = \frac{m_p}{A_f \cdot \rho_p} \qquad (11)$$

where: m_p is the total mass of particles on the filter, A_f is the filtration area (area of the open channels), and ρ_p is the bulk density of the particle layer. The face velocity can also be calculated from the continuity equation for the flow of exhaust through the filter:

$$m_g = \frac{p_{exh}}{R\ T_{exh}} \cdot v \cdot A_f \qquad (12)$$

Substituting Equations (11) and (12) into Darcy's law for the pressure drop contribution due to the particles, one obtains:

$$dp = \frac{\dot{m}_g \cdot m_p \cdot R \cdot T_{exh}}{p_{exh} \cdot \mu \cdot A_f^2} \cdot \frac{1}{\rho_p \cdot \alpha} \qquad (13)$$

In Equation (13), it can be seen that the problem with the uncertainty concerning the thickness of the particles has been replaced by the uncertainty of the bulk density of the particle layer. All of the parameters with the exception of the density and the permeability can be re[illegible]ly measured during engine testing. It can also be seen that it is actually the product of the permeability and the density that determines the pressure loss for a given flow rate and particle loading.

Consequently, in the following results, the parameter determined will be the product of the density and the permeability. It is possible to determine the density of the particle layer, but it involves the same difficulties as the measurement of the thickness.

RESULTS

Experimental measurements for the flow properties were obtained by performing a series of experiments on a diesel engine run at different constant speeds and loads and then collecting particles for two types of filter materials, SiC and Cordierite. Specifications of the engine and filters used are given in Tables 3 and 4 respectively. The base materials correspond to those in Table 1. The physical properties of the two filter materials are comparable in terms of mean pore size and porosity. Both filters were packed into stainless steel cylinders and surrounded by conventional packaging material and were equipped with quick-connect flanges for frequent removal.

The Cordierite filter was constructed in a single unit, while the SiC filter was composed of 4 pie shaped segments with the packing material pressed between the segments (1).

Bore	93.0 mm
Stroke	88.4 mm
Cylinders	4
Displacement	2.4 liter
Combustion System	Indirect Injection

Table 3. Engine parameters for the particle collection experiments

In the experiments, identical speed and load conditions were tested for each filter material. Engine speeds were varied from 1500 rpm to 3000 rpm, and three load levels were used: 35, 65, and 95 N-m corresponding to Brake Mean Effective Pressures of 183, 340, and 497 kPa. At the highest speed, the highest load was not used since intention of the experiments was only to look at the collection of particles and not the regeneration of the filters, and there was concern that some regeneration would occur.

No specific limit was set on the engine back pressure, and the experiments were conducted in a manner such that the pressure rise as a function of time was linear and that the rate of increase of pressure with time could be accurately determined. Even with high

Filter Unit Property	SiC	Cordierite
Diameter - mm	170	144
Length - mm	125	152
Volume - liter	2.84	2.48
Cell size - mm	3.54	2.54
Wall Thickness - mm	1.0	0.63
Filtration Area - m^2	1.19	1.56

Table 4. Properties of the filters used in the particle collection experiments.

back pressures, the pressure time curves generally increased linearly, and no dramatic pressure increases were observed at the end of the collection process.

For each operating condition, the engine was run the same length of time for both filter materials. Comparative filtration efficiencies were determined by dismounting the filters after each run and then weighing them. An electric scale was used that has the ability to weigh up to 11 kg to an accuracy of ± 0.1 gram. The SiC filter assembly weighed 6 kg while the Cordierite assembly weighed 4.9 kg.

Following the weighing, the filters were then regenerated using an electrically heated oven equipped with a small blower for compressed air. After heating to a predetermined temperature, air was blown through the filters to regenerate them. The effectiveness of the regeneration was checked by monitoring the weight of the filter after each regeneration.

A summary of the collected particle masses on the two filters is shown in Figure 8, where the mass collected on the SiC filter is plotted as a function of the mass collected on the Cordierite filter. The straight line shown represents equal mass on both filters. In general, it can be observed that there is no significant difference in the collection efficiency. There are uncertainties and errors associated with the disassembly and weighing procedure, it was determined that the filter weights were accurate to about ± 3 g.

Figure 9 shows typical exhaust pressure and exhaust temperature measurements as of function of time for the filter materials for an engine speed of 1500 rpm and a BMEP of 340 kPa, while Figure 10 shows similar results for a higher speed of 3000 rpm and a lower BMEP of 183 kPa. It should be pointed out that the pressure rise shown is the increase above the pressure drop caused by a clean filter. The clean filter pressure drops have been calculated using the results from Figure 5.

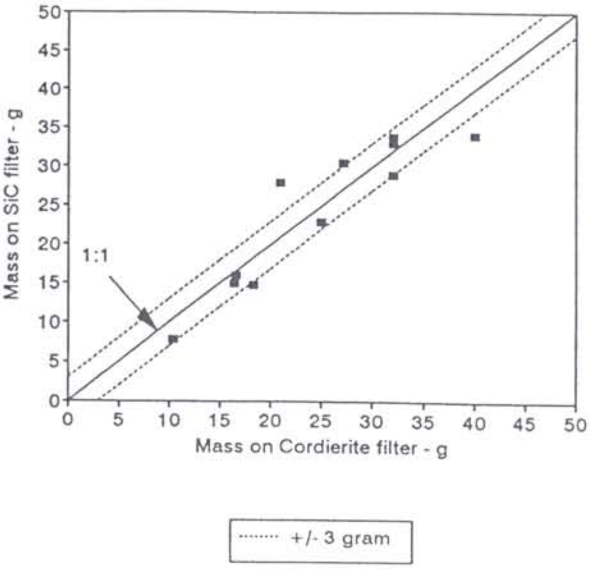

Figure 8. Comparison of the mass of particles collected on the SiC and Cordierite filters for identical engine operating conditions.

These results indicate that for identical engine conditions, the SiC filter has a lower pressure drop throughout the entire collection process. This is found even though the SiC filtration area is 24 % smaller than that of the Cordierite, and the its wall thickness is 65 % larger than that of the Cordierite filter.

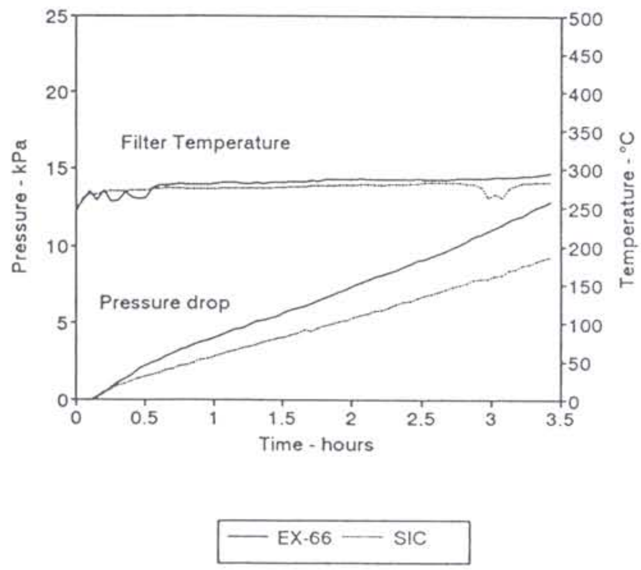

Figure 9. Exhaust temperatures and pressures during particle buildup at 1500 rpm and a BMEP of 340 kPa.

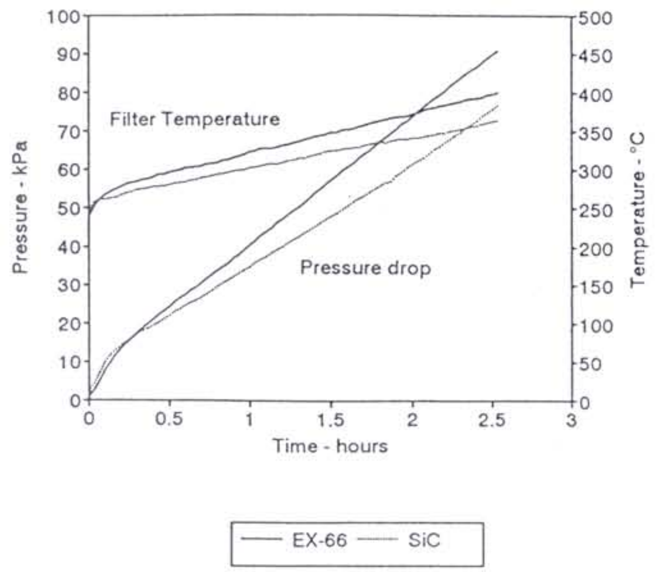

Figure 10. Exhaust temperatures and pressures during particle buildup at 3000 rpm and an BMEP of 183 kPa.

The results in Figures 9 and 10 encompass a wide range of pressures, including pressures considerably higher than those which would normally be accepted in typical operation. Similar results have been shown by Howitt and Montierth (10) in their investigation of the behavior of different types of Cordierite filter materials. In agreement with the results of Reference (9), there is an initial portion of the curve where the rate of pressure rise is high, after which the rate of pressure rise becomes nearly constant. The initial portion of the pressure development is thought to be connected to the initial build up of the particle layer on or partly in the filter material, but has not been investigated in detail.

These results are typical of those found for the entire range of operating conditions. This is shown in Figure 11, which is a plot of the rate of pressure rise under particle collection for the SiC filter as a function of the rate of pressure rise for the Cordierite filter. The pressure rise shown is the rate of change of pressure with respect to time in the region where the pressure rise curve is stable. It can be seen that in all cases the pressure rise is lower for the SiC filter than the Cordierite filter in spite of a smaller filtration area. From Figure 8, it can be seen that the particle mass collected on each filter is essentially the same at each condition.

According to Equation (13), one would expect a linear relationship for the pressure rise as a function of the product of the flow rate and particle mass divided by the product of the exhaust gas density, the gas viscosity and the square of the filtration area. A plot of the results for the particles collected on the two filters at 1500 rpm is given in Figure 12. Included in the curves are points taken from measurements of cold loaded filters on the flow bench.

It is clear from Figure 12 that there is a relationship of the form expected from Equation (13). If the product $\rho_p\alpha$ for the particle layer is constant, it can be determined from the slope of the curve in Figure 12. It is also possible, however, to determine the value of the $\rho_p\alpha$ product for each data point. This procedure should be more general, since it would allow for variations in the value of $\rho_p\alpha$.

These results are given in Figure 13 which shows the product $\rho_p\alpha$ as a function of the pressure drop across the particle layer. The conditions shown include all the engine operating points.

There is a noticeable scatter in the data, particularly at the low pressure drops corresponding to low particle loading and, therefore, a greater relative uncertainty in the particle mass. In spite of the scatter, there are two observations which can be made. The value of the product $\rho_p\alpha$ for the particles collected on the SiC filter material is generally greater than the value for the corresponding product for the particles collected on the Cordierite filter. This is a reflection of the results for the rate of pressure rise during particle collection, which for SiC show lower pressure drops due to the particle layer for equivalent loadings, but with a smaller filtration area. The particle layer for particles collected on the SiC substrate has a lower flow resistance than that collected on the Cordierite EX-66 substrate which

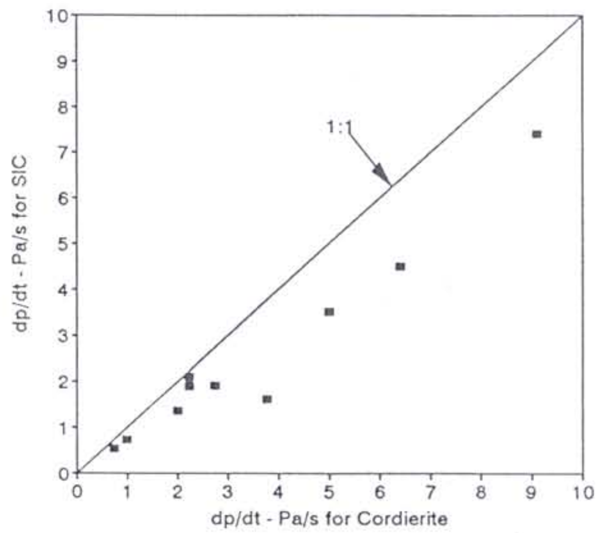

Figure 11. Comparison of the pressure difference due to particle accumulation for particles collected on the two filter materials.

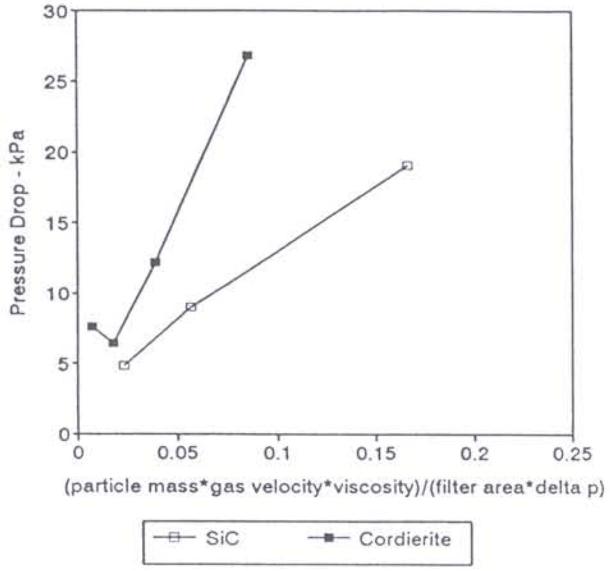

Figure 12. Pressure difference across the particle layer as a function of the product of particle mass, face gas velocity and viscosity divided by the product of the filter area and the pressure difference (see Equation (13) in the text).

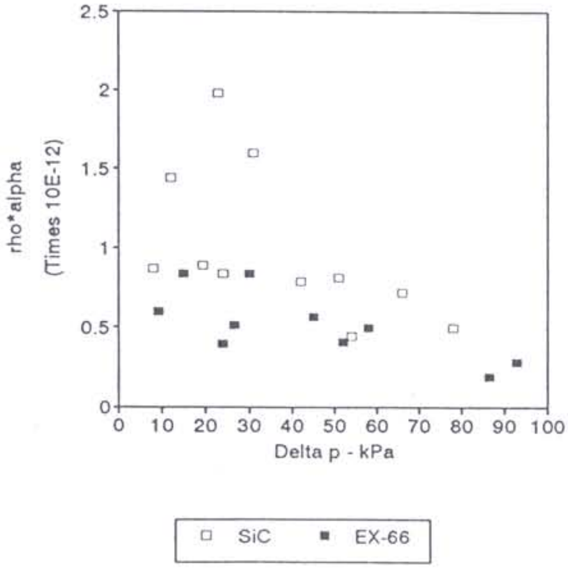

Figure 13. The product of the bulk density and permeability, $\rho_p\alpha$, of the particle layer as a function of the pressure difference reached during collection for particles collected on the two filter materials.

is of a comparable pore size and porosity. The results have been given in terms of the permeability and the particle density, which are general factors, and can be easily related to other filter constructions using the same filter materials.

This is not to say that $\rho_p\alpha$ is independent of the underlying filter structure or the conditions under which the particle layer has been created. This is illustrated by the second observation concerning Figure 13. There is a general tendency for the product $\rho_p\alpha$ to decrease as the pressure difference across the particle layer increases. This occurs for the particles collected on both materials, and can be construed as a compression of the particle layer. If this is the case, then one would expect the bulk density of the particle layer to increase with the pressure difference across it.

As mentioned previously, determination of the particle bulk density is difficult and involves the destruction of the filter sample. A few determinations have been made. For the Cordierite material with particles collected up to a pressure difference of 45 kPa, a particle layer bulk density of 0.12 g/cm^3 was found. For the SiC material with particles collected up to a pressure difference of 25 kPa, a particle layer bulk density of 0.09 g/cm^3 was found. Howitt and Montierth (10) report a value of 0.05 to 0.06 g/cm^3 in studies of Cordierite materials with pressures under 15 kPa. These results give an indication that the particle layer bulk density increases with increasing pressure difference. The interpretation of the bulk density results should be treated with caution, because in addition to differing pressures, the results were obtained for particles collected on at least three different filter materials.

Since the results of Figure 13 indicate a decrease in the product $\rho_p\alpha$ with increasing pressure difference, and increase in the density would have to be compensated by an even larger relative reduction in the permeability. However, as shown previously, it is only the product of the bulk density and the permeability which is needed in order to determine the pressure difference over the particle layer.

The reason why the permeability-bulk density product is greater for the SiC structure is not known with certainty. It is thought to be due to the more uniform pore size distribution of the SiC filter material, which is made of a limited size range of particles. This gives a more consistent open structure, an limits the number of large blind pores in the structure. This can be seen in Figures 1 and 2.

It has been observed that for the Cordierite material, that there are a few very large pores in the wall material that are filled early, and then the particle layer collects outside the filter material. For the SiC material with a comparable mean pore size, the very large pores are not found, and so initially it is expected that the particles collect to some unknown depth in the filter material. During this time, the flow resistance to the particle layer is lower than for the Cordierite. This is supported by the observation that when one attempts to remove the particle layer from the filters, the SiC particle layer holds more tightly to the filter surface, and is harder to remove than the particle layer on the Cordierite material.

Eventually, both materials would contain all the particles which their structures would allow, and then the particle layer would be built up away from the surface of the base material. In this case, one would expect that the differences between base material structure would have less of an impact on the flow resistance of the particle layer. Figure 13 suggests that this is the case for large pressure drops, since the data points for the two materials tend to be closer together than for the smaller pressure drops.

CONCLUSIONS

The relationship between pressure drop and flow has been established for filter materials made of SiC and of Cordierite with comparable physical parameters. This relationship gives the friction factor for the filter material as a function of a Reynolds number bases on an equivalent spherical diameter which is proportional to the square root of the permeability. The results are consistent with literature trends for Cordierite filters with different physical characteristics.

The range of validity of Darcy's law has been established for the filter materials tested. The permeabilities of the filter materials have been identified, and their connection to the relationship between a friction factor and the Reynolds number established.

Flow characteristics of the layer of particles collected on the filter materials have also been established. It is shown that the product of the bulk density of the particles and the permeability of the particle layer is adequate to describe the pressure losses through the particle layer. This product was found to be dependent on the maximum pressure at which the particles are collected and the type of filter material on which the particles are collected.

It was found that not only is the permeability larger for the base SiC material, but that the permeability of the layer of particles collected on the material is higher than that of the Cordierite, even for large particle loading.

ACKNOWLEDGEMENTS

The authors would like to express their appreciation to Henrik G. Petersen and Sten Ankjær for their assistance in obtaining experimental data.

REFERENCES

1. Stobbe, P., J. W. Høj, H. G. Petersen, S. C. Sorenson, "SiC as a Substrate for Diesel Particulate Filters", SAE paper 9302495, 1993.

2. Itoh, A. et al. "Study of SiC Application to Diesel Particulate Filter (Part 1): Material Development", SAE paper 930360, 1993.

3. Itoh, A. et al. "Study of SiC Application to Diesel Particulate Filter (Part 2): Engine Test Results", SAE paper 930360, 1993.

4. Goto, Y., T. Abe. T. Sato, M. Hauashida, "Study on regeneration of Diesel Particle Trapper by Electrical Self-Heating Type Filter", SAE Paper 920140, in Diesel Particulate Control, Trap and Filtration Systems, SAE SP-896, 1992.

5. Gulati, T. S., and Sherwood, D. L., "Dynamic fatigue for Cordierite Ceramic Wall-Flow Diesel Filters", SAE paper 910135.

6. Dullien, F. A. L. Porous Media Fluid Transport and Pore Structure, Academic Press, Inc., New York, 1979.

7. W. H. Lipkea, J. H. Johnson, C. T. Vuk, "The Physical and Chemical Character of Diesel Particulate Emissions - Measurements Techniques and Fundamental Considerations", SAE paper 780108, 1978.

8. Konstandopoulos, A. G. and J. H. Johnson, "Wall-Flow Diesel Particulate Filters--Their Pressure Drop and Collection Efficiency", SAE Paper 890405, in Developments in Diesel Particulate Control Systems, SAE Special Publication SP-775, 1989.

9. Mogaka, Z. N., V. W. Wong, and S. M. Shahed, "Performance and Regeneration Characteristics of a Cellular Ceramic Diesel Particulate Trap", SAE Transactions, paper 820272, 19822.

10. Howitt, J. S., Montierth, M. R., "Cellular Ceramic Diesel Particulate Filter", SAE paper 810114, 1981.